

# FuXi- $\gamma$ : Efficient Sequential Recommendation with Exponential-Power Temporal Encoder and Diagonal-Sparse Positional Mechanism

Dezhi Yi

dezhi.yi@mail.nankai.edu.cn  
College of Computer Science, DISSec  
Nankai University  
Tianjin, China

Wei Guo

guowei67@huawei.com  
Huawei Technologies  
Shanghai, China

Wenyang Cui

cuiwenyang@mail.nankai.edu.cn  
College of Computer Science, DISSec  
Nankai University  
Tianjin, China

Wenxuan He

wxhe@mail.nankai.edu.cn  
College of Computer Science, DISSec  
Nankai University  
Tianjin, China

Huifeng Guo

huifeng.guo@huawei.com  
Huawei Technologies  
Shenzhen, China

Yong Liu

liu.yong6@huawei.com  
Huawei Technologies  
Shanghai, China

Zhenhua Dong

dongzhenhua@huawei.com  
Huawei Technologies  
Shenzhen, China

Ye Lu\*

luye@nankai.edu.cn  
College of Computer Science, DISSec  
Nankai University  
Tianjin, China

## Abstract

Sequential recommendation aims to model users' evolving preferences based on their historical interactions. Recent advances leverage Transformer-based architectures to capture global dependencies, but existing methods often suffer from high computational overhead, primarily due to discontinuous memory access in temporal encoding and dense attention over long sequences. To address these limitations, we propose FuXi- $\gamma$ , a novel sequential recommendation framework that improves both effectiveness and efficiency through principled architectural design. FuXi- $\gamma$  adopts a decoder-only Transformer structure and introduces two key innovations: (1) An exponential-power temporal encoder that encodes relative temporal intervals using a tunable exponential decay function inspired by the Ebbinghaus forgetting curve. This encoder enables flexible modeling of both short-term and long-term preferences while maintaining high efficiency through continuous memory access and pure matrix operations. (2) A diagonal-sparse positional mechanism that prunes low-contribution attention blocks using a diagonal-sliding strategy guided by the persymmetry of Toeplitz matrix. Extensive experiments on four real-world datasets demonstrate that FuXi- $\gamma$  achieves state-of-the-art performance in recommendation quality, while accelerating training by up to 4.74 $\times$  and

inference by up to 6.18 $\times$ , making it a practical and scalable solution for long-sequence recommendation. Our code is available at <https://github.com/Yeedzhi/FuXi-gamma>.

## CCS Concepts

• Information systems  $\rightarrow$  Recommender systems.

## Keywords

Sequential Recommendation, Temporal Encoder, Sparse Positional Mechanism

## ACM Reference Format:

Dezhi Yi, Wei Guo, Wenyang Cui, Wenxuan He, Huifeng Guo, Yong Liu, Zhenhua Dong, and Ye Lu. 2026. FuXi- $\gamma$ : Efficient Sequential Recommendation with Exponential-Power Temporal Encoder and Diagonal-Sparse Positional Mechanism. In *Proceedings of the 32nd ACM SIGKDD Conference on Knowledge Discovery and Data Mining V.1 (KDD '26)*, August 09–13, 2026, Jeju Island, Republic of Korea. ACM, New York, NY, USA, 12 pages. <https://doi.org/10.1145/3770854.3780176>

## 1 Introduction

Sequential recommendation aims to predict users' next interaction based on their historical behavior sequences [22, 43, 52]. Accurate predictions improve user experience and drive substantial commercial value [21, 32, 47]. The training efficiency of recommendation models affects their update frequency and service freshness, while inference efficiency impacts system latency and deployment cost [29, 30, 46]. Hence, designing recommendation frameworks that are both effective and efficient is a core challenge.

Recent advances in generative recommendation models [1, 52, 55] leverage autoregressive architectures to achieve superior performance and scaling effects compared to traditional methods [16, 22,

\*Corresponding author.



This work is licensed under a Creative Commons Attribution 4.0 International License. *KDD '26, Jeju Island, Republic of Korea*  
© 2026 Copyright held by the owner/author(s).  
ACM ISBN 979-8-4007-2258-5/2026/08  
<https://doi.org/10.1145/3770854.3780176>

43]. However, these models often introduce efficiency bottlenecks due to architectural complexity. For example, although HSTU [55] improves HR@10 by 55.18% over SASRec [22], it suffers from a 3.21× slowdown in training efficiency. FuXi- $\alpha$  [52] further improves HR@10 by 5.66% over HSTU but incurs an additional 9.63% efficiency loss. Such inefficiency forces production systems to reduce model size to meet latency requirements, weakening the scaling benefits of the autoregressive paradigm.

A primary efficiency bottleneck in sequential recommendation lies in temporal encoding module. Temporal information is essential for capturing the dynamics of user preferences over time, which is fundamental to modeling interest patterns [2, 28, 51]. However, temporal encoders in existing state-of-the-art frameworks often conflict with parallel hardware due to irregular and fragmented memory access, severely limiting computational efficiency. For example, both HSTU [55] and FuXi- $\alpha$  [52] employ a T5-style bucket-based encoding scheme [37], where relative temporal intervals are log-transformed and discretized into distinct indices for bucket lookup. This operation pattern results in  $n^2$  non-contiguous and unstructured memory accesses for a sequence of length  $n$ , posing a major obstacle to parallel execution on modern hardware. Although FuXi- $\beta$  [53] introduces an inverse-proportion decay function to alleviate some of these issues, both approaches lack grounding in cognitive principles, limiting their expressiveness and explainability.

Another overlooked inefficiency stems from positional encoding module. Modern frameworks introduce relative positional encoding even when absolute positional embedding and temporal signal are already available. For example, FuXi- $\alpha$  [52] and FuXi- $\beta$  [53] incorporate positional encoding as a separate attention channel with  $O(n^2)$  complexity, which becomes an efficiency bottleneck for long sequences. Recent advances in block-sparse semantic attention [8, 20, 27, 50] offer promising solutions, but have yet to be explored in the context of positional attention in recommendation.

To address dual challenges of efficiency and effectiveness in modeling user interests, we propose a novel sequential recommendation framework named FuXi- $\gamma$ . Building upon FuXi- $\beta$  [53], FuXi- $\gamma$  adopts an autoregressive architecture with dual attention channels for temporal and positional modeling. We introduce two key innovations: (1) An exponential-power temporal encoder, inspired by the Ebbinghaus forgetting curve [5], which models time-aware user interest decay through a continuous, fully matrix-based formulation. This cognitively motivated design offers strong expressiveness and hardware-friendly execution, yielding up to **11.00×** speedup over the bucket-based encoder and significant gains in recommendation performance. (2) A diagonal-sparse positional mechanism, which identifies and prunes low-contribution attention blocks based on importance scoring on the leftmost column, reducing positional attention overhead by **74.56%** while preserving recommendation quality. Together with practical optimizations such as data type pre-conversion, FuXi- $\gamma$  achieves up to **4.74×** and **6.18×** improvements in training and inference efficiency, respectively, while consistently outperforming state-of-the-art baselines across multiple datasets.

Our main contributions are summarized as follows:

- We propose a novel sequential recommendation framework, FuXi- $\gamma$ , that enhances both effectiveness and efficiency, particularly in scenarios involving long sequences.
- We design an exponential-power temporal encoder that models user interest decay through a tunable exponential function. It offers flexibility to adapt to diverse behavioral patterns and achieves high efficiency through regular memory access and pure matrix operations.
- We introduce a diagonal-sparse positional mechanism that prunes redundant attention blocks, substantially reducing computational overhead while preserving recommendation accuracy.
- We conduct extensive experiments on four real-world datasets, demonstrating that FuXi- $\gamma$  achieves state-of-the-art performance. On a large-scale industrial music dataset, FuXi- $\gamma$  achieves improvements of **25.06%** in HR@10 and **42.86%** in NDCG@10 over strong autoregressive baselines.

## 2 Related Work

### 2.1 Sequential Recommendation

Sequential recommendation aims to predict users' future preferences based on their interaction sequences. Early methods employ probabilistic models, such as Markov Chains [39] and session-based kNN [15, 17], to capture short-term transitions. Subsequent deep learning approaches model higher-order dependencies through CNNs [44], RNNs [34], and GRU-based architecture [16]. With the introduction of Transformer [45], global dependency modeling becomes possible via self-attention. SASRec [22] uses multi-head self-attention to identify important items. BERT4Rec [43] leverages bidirectional encoding for improved prediction. Further extensions explore more complex settings, including cross-domain [60], multi-modal [57], and multi-behavior scenarios [42].

Traditional frameworks typically follow a ranking-based formulation, which limits their scalability and adaptability. Generative recommendation reframes the task as sequence generation, enabling unified, end-to-end modeling. TIGER [38] pioneers generative recommendation for zero-shot scenarios. HLLM [1] tokenizes item IDs for autoregressive modeling with large language models. HSTU [55] scales recommendation using Transformer-based generation. FuXi- $\alpha$  [52] introduces a three-channel design to separately model semantic, temporal, and positional features, while FuXi- $\beta$  [53] improves efficiency by removing semantic modeling.

Despite recent progress, balancing effectiveness and efficiency remains a core challenge. To this end, we propose FuXi- $\gamma$  that integrates a cognitively inspired temporal encoder and a sparse positional mechanism to improve both performance and scalability.

### 2.2 Temporal Encoder

Temporal information plays a crucial role in capturing the evolving nature of user interests. Prior works explore various strategies, such as encoder-decoder timestamp modeling [59], joint learning of temporal patterns [51], and multi-granularity temporal embeddings [2]. TiSASRec [28] explicitly incorporates both absolute positions and relative temporal intervals. Time2Vec [23] represents temporal signals through sinusoidal and linear activations. More recently, generative recommendation models like HSTU [55] and FuXi- $\alpha$  [52] adopt T5-style bucket encodings [37] to discretize relative temporal intervals. Despite effectiveness, the bucket-based method introduces discontinuous memory access and poor hardware utilization, resulting in substantial efficiency bottlenecks, particularly

for long sequences. FuXi- $\beta$  [53] replaces bucketing with an inverse-proportional decay function, offering improved efficiency. However, its fixed decay pattern lacks adaptability across different application scenarios, limiting modeling flexibility.

To overcome these limitations, we propose an exponential-power temporal encoder inspired by the Ebbinghaus forgetting curve [5]. The design enables flexible modeling of temporal decay patterns and maintains efficient, hardware-friendly continuous memory access.

### 2.3 Positional Encoder

Positional encoding provides contextual information for sequence modeling tasks. Existing approaches can be broadly classified into absolute and relative encoding methods. Absolute encodings directly incorporate positional vectors into item representations, typically implemented using either fixed sinusoidal functions [45] or learnable embeddings [9]. Relative encodings [3, 14, 19, 24, 37, 40] model pairwise item distances by learning weights associated with relative positional offsets. Recent generative recommendation models often combine both encoding types, integrating relative encoding either as an additive bias in the semantic channel [55] or as a separate attention matrix in an independent channel [52, 53].

Following FuXi- $\alpha$  [52] and FuXi- $\beta$  [53], we adopt relative positional encoding as a separate attention matrix. However, we observe that positional information is already partially captured by the embedding layer and the temporal encoder, introducing redundancy. To mitigate this, we design a diagonal-sparse pruning method applied after training. This method removes low-contribution blocks from the positional attention matrix, significantly reducing computation overhead while preserving recommendation accuracy.

## 3 Methodology

In this section, we begin by formally defining the next-item sequential recommendation task. We then present the overall architecture of FuXi- $\gamma$ , followed by a detailed description of its core components.

### 3.1 Problem Statement

The primary objective of sequential recommendation is to predict the next item a user is likely to interact with, conditioned on their historical interaction sequence. Formally, let  $\mathcal{U} = \{u_1, u_2, \dots, u_{|\mathcal{U}|}\}$  denote the set of users, and  $\mathcal{V} = \{v_1, v_2, \dots, v_{|\mathcal{V}|}\}$  the set of items. For each user  $u \in \mathcal{U}$ , the interaction history is represented as a time-ordered sequence  $S_u = [(v_1^{(u)}, t_1^{(u)}), (v_2^{(u)}, t_2^{(u)}), \dots, (v_{n_u}^{(u)}, t_{n_u}^{(u)})]$ , where each tuple  $(v_i^{(u)}, t_i^{(u)})$  corresponds to an item interacted with at timestamp  $t_i^{(u)}$ . The goal is to predict the subsequent item  $v_{n_u+1}^{(u)}$  that user  $u$  will interact with, given their historical sequence  $S_u$ . This task is typically formulated as estimating the conditional probability distribution over the item space:  $P(v_{n_u+1}^{(u)} = v \mid S_u), \forall v \in \mathcal{V}$ .

During training, the model is optimized to predict the next item  $v_{i+1}^{(u)}$  at each position  $i$  along the sequence  $S_u$ . Thus the desired output sequence corresponds to  $[v_2^{(u)}, v_3^{(u)}, \dots, v_{n_u+1}^{(u)}]$  [22].

### 3.2 Overall Architecture

The overall architecture of FuXi- $\gamma$  is illustrated in Figure 1. Following the design of FuXi- $\beta$  [53], FuXi- $\gamma$  adopts a decoder-only

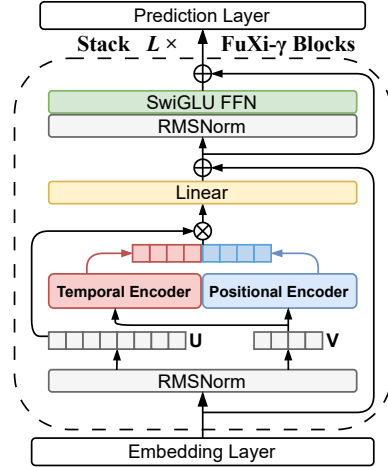


Figure 1: Overall architecture of FuXi- $\gamma$ .

Transformer architecture without query-key attention, aiming to streamline computation while preserving modeling capacity. Specifically, FuXi- $\gamma$  consists of three components: (1) Embedding Layer: Encodes input items with learned item embeddings and incorporates absolute positional information. (2) FuXi- $\gamma$  Block: Capture user interest patterns via dual-channel self-attention layer and SwiGLU FFN. (3) Prediction Layer: Computes the probability distribution over the item vocabulary for the next-item prediction.

**3.2.1 Embedding Layer.** To address the variability in user interaction sequence lengths, we normalize each user's interaction history to a fixed length  $n$  prior to the embedding layer. Sequences longer than  $n$  are truncated, while shorter sequences are padded with a special "padding item". Each item  $v \in \mathcal{V}$  is mapped to a  $d$ -dimensional vector via a learnable embedding matrix  $E \in \mathbb{R}^{|\mathcal{V}| \times d}$ . In addition, we incorporate absolute positional information by adding learnable positional embeddings. Let  $e_i$  and  $p_i$  denote the item embedding and positional embedding of the  $i$ -th position, respectively. For a user sequence  $S_u$ , the output of the embedding layer is given by:

$$X^0 = [e_1^{(u)} + p_1, \dots, e_{n_u}^{(u)} + p_{n_u}, \mathbf{0}, \dots, \mathbf{0}], \quad (1)$$

where vectors  $\mathbf{0}$  correspond to padding positions from  $n_u + 1$  to  $n$ .

The resulting embedding  $X^0$  is subsequently passed through a stack of FuXi- $\gamma$  blocks to capture user interest patterns. The design details of FuXi- $\gamma$  block are described in Section 3.3.

**3.2.2 Prediction Layer & Optimization Objective.** After passing through  $L$  stacked FuXi- $\gamma$  blocks, each position in the sequence encodes sufficient contextual information from previously interacted items. To generate the prediction, we project the final hidden representation onto the item space by computing dot product with the transpose of input embedding matrix, followed by a softmax function to obtain a probability distribution over all candidate items:

$$P(v_i^{(u)} = v \mid [(v_1^{(u)}, t_1^{(u)}), \dots, (v_{i-1}^{(u)}, t_{i-1}^{(u)})]) = \text{Softmax}(x^L E^T)_v, \quad (2)$$

where  $x^L$  denotes the final-layer representation at position  $i - 1$ , and  $E$  is the input embedding matrix. To improve training efficiency, we adopt the sampled softmax loss, where the softmax is computed over the true item and  $N$  randomly sampled negative items [25].

### 3.3 FuXi- $\gamma$ Block

FuXi- $\gamma$  block comprises two components: a dual-channel self-attention layer and a SwiGLU feed-forward network (FFN) [41]. To improve training stability, we adopt a pre-normalization [10] strategy, applying layer normalization before each sub-layer computation.

**3.3.1 Dual-Channel Self-Attention Layer.** This layer decouples representation learning into two distinct channels: a temporal channel and a positional channel. This design enables each channel's encoder to specialize in capturing different aspects of the sequence information. Then, we adopt a post-mixing strategy via point-wise interaction and linear projection to aggregate signals.

Let  $X \in \mathbb{R}^{n \times d}$  denote the input embedding to one FuXi- $\gamma$  block. We first construct two projection representations of input sequence:

$$U, V = \text{Split}(\phi(\text{RMSNorm}(X)W_{uv})), \quad (3)$$

where RMSNorm denotes root mean square layer normalization [56],  $W_{uv} \in \mathbb{R}^{d \times 3d}$  is a learnable matrix,  $\phi$  denotes SiLU nonlinear transformation [6],  $U \in \mathbb{R}^{n \times 2d}$  and  $V \in \mathbb{R}^{n \times d}$  are two projected outputs.

To simplify computation and improve efficiency, we share  $V$  between temporal and positional encoders to learn user interests. Then the outputs of two encoders are concatenated and mixed with  $U$  via Hadamard product to enable explicit 2-order interactions:

$$I = \text{RMSNorm}(\text{Concat}(A_{ts}V, W_{pos}V)) \odot U, \quad (4)$$

where  $A_{ts} \in \mathbb{R}^{n \times n}$  is a temporal attention matrix constructed based on relative temporal intervals (see Section 3.4.1 for design details);  $W_{pos} \in \mathbb{R}^{n \times n}$  is a learnable positional encoding matrix, where  $W_{pos}^{i,j}$  denotes the attention weight for relative positional offset  $i - j$  and satisfies  $W_{pos}^{i,j} = W_{pos}^{i+m,j+m}$ , i.e.,  $W_{pos}$  is a Toeplitz matrix.

Finally, we pass the interaction result  $I \in \mathbb{R}^{n \times 2d}$  through a linear layer to aggregate temporal and positional signals, and introduce a residual connection [13] to maintain original sequence information:

$$O = IW_o + b + X, \quad (5)$$

where  $W_o \in \mathbb{R}^{2d \times d}$  and  $b \in \mathbb{R}^d$  are learnable parameters.

**3.3.2 SwiGLU FFN.** Each dual-channel self-attention layer is followed by a SwiGLU FFN, which further refines the representation through implicit interactions. To preserve the flow of gradients and enable deep modeling, we incorporate a residual connection around the FFN. The computations are formally defined as:

$$\begin{aligned} O' &= \text{RMSNorm}(O), \\ H &= (\phi(O'W_1) \odot (O'W_2))W_3 + O, \end{aligned} \quad (6)$$

where  $\phi$  is SiLU activation,  $W_1, W_2 \in \mathbb{R}^{d \times d_{\text{FFN}}}$  and  $W_3 \in \mathbb{R}^{d_{\text{FFN}} \times d}$  are learnable weights,  $H \in \mathbb{R}^{n \times d}$  is the final output of FuXi- $\gamma$  block.

### 3.4 Exponential-Power Temporal Encoder

Effectively and efficiently capturing the evolving nature of user interests over time is a key challenge. To address this problem, we propose an exponential-power temporal encoder that utilizes a continuous and tunable decay mechanism, offering both strong modeling capabilities and high computational efficiency.

**3.4.1 Algorithm Design.** Motivated by the intuition that recent interactions better reflect users' current interests, we impose a monotonic decay pattern on temporal attention weights: smaller temporal intervals receive higher weights, while larger intervals receive lower weights. Inspired by the Ebbinghaus forgetting curve [5], which describes human memory decays exponentially over time, we adopt a tunable exponential function to model the temporal decay in user preferences. First, we represent temporal intervals within a user's interaction sequence as pairwise differences between item timestamps. Specifically, we construct a relative temporal matrix  $T \in \mathbb{N}^{n \times n}$  for each sequence, where  $T^{i,j}$  denotes the absolute difference between the timestamps of the  $i$ -th and  $j$ -th items:  $T^{i,j} = |t_i - t_j|$ . To reduce computation and memory cost, this preprocessing is performed only once, and the resulting  $T$  is shared across all temporal encoders. Then, we apply a nonlinear transformation to  $T$  using a power function. This design prevents insufficient learning of long-term user preferences that can occur when excessively long temporal intervals produce very weak signals. Finally, we adopt an exponential function to model the decay of user interests over time. Formally, the temporal attention matrix  $A_{ts} \in \mathbb{R}^{n \times n}$  used in Section 3.3.1 is defined as:

$$A_{ts} = \alpha \cdot \gamma^{T^\beta}, \quad \text{i.e.,} \quad A_{ts}^{i,j} = \alpha \cdot \gamma^{|t_i - t_j|^\beta}, \quad \gamma \in (0, 1), \quad (7)$$

where  $\alpha \in \mathbb{R}$  is a learnable parameter representing the base interest intensity,  $\beta \in \mathbb{R}$  is a learnable parameter controlling the nonlinearity of scaling transformation, and  $\gamma \in (0, 1)$  is a decay parameter that governs the rate of interest attenuation. A smaller  $\gamma$  induces faster decay, emphasizing short-term patterns, whereas a larger  $\gamma$  preserves more long-term signals. This design offers flexibility across diverse user behaviors and application scenarios, enabling the model to capture both short-term and long-term preferences in a simple yet expressive manner.

**3.4.2 Pre-Conversion of Data Type.** In Equation 7, the parameters  $\alpha$ ,  $\beta$ , and  $\gamma$  are represented in float32, while the relative temporal matrix  $T$  is originally in int64. Due to the inconsistency of data types, computing  $T^\beta$  implicitly introduces type casting at runtime, which incurs additional time overhead and becomes more costly when repeated across multiple layers. To mitigate this issue, we explicitly cast  $T$  to float32 during preprocessing. This pre-conversion ensures that all subsequent operations, such as power and exponential calculations, are performed using the same data type, thereby avoiding runtime casting and improving computational efficiency. This simple optimization brings notable performance gains: (1) The execution time of our exponential-power temporal encoder is reduced by 64.82%. (2) Overall FuXi- $\gamma$  achieves an additional 12.61% speedup and 5.08% reduction in memory usage during training, and a 15.53% speedup and 6.98% memory reduction during inference.

**3.4.3 Analysis.** Our proposed exponential-power temporal encoder achieves strong performance in both architectural compatibility and computational efficiency (see Section 4.3 for details). Existing bucket-based method, as used in HSTU [55] and FuXi- $\alpha$  [52], applies logarithmic transformations to temporal intervals and then maps them into discrete indices for bucket lookup. Although this approach offers some modeling flexibility, it suffers from several key limitations: (1) The design does not reflect how user interests evolve over time. (2) Coarse-grained discretization leads to a loss of

detail, as different temporal intervals may fall into the same bucket. (3) Most importantly, the irregular memory access during bucket lookup creates a critical efficiency bottleneck, especially when handling long sequences. FuXi- $\beta$  [53] proposes an inverse-proportion function to represent temporal decay, which helps reduce memory access overhead and partly captures interest attenuation. However, it lacks adaptability due to the untunable decay pattern, which overly favors recent interactions and limits flexibility in modeling longer-term user preferences. In contrast, our exponential-power encoder is inspired by cognitive memory theory and operates entirely through standard matrix computations. This design enables more accurate modeling of adaptive-range interests and ensures smooth and efficient execution on modern hardware.

### 3.5 Diagonal-Sparse Positional Mechanism

Positional information is explicitly encoded in the embedding layer and implicitly reflected through temporal signals. Therefore, we identify and prune redundant weights in relative positional attention, further enhancing the inference performance of FuXi- $\gamma$ . Specifically, we design the diagonal-sparse positional mechanism, which consists of three steps: (1) Block-level division of the positional attention map. (2) Importance scoring of each block. (3) Selection of important blocks for sparse attention computation.

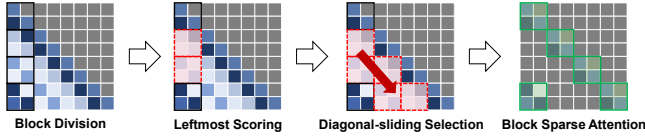


**Figure 2: Illustration of diagonal-sparse positional mechanism.** In this example, sequence length  $n = 8$ , stride size  $s = 2$ , and configured pruning ratio  $\tau = 50\%$ . Red Blocks are pruned due to lower importance scores. Only the remaining green blocks participate in positional attention computation.

**3.5.1 Block Division.** Element-level unstructured pruning offers accuracy advantages but incurs considerable overhead in hardware deployment. Row-level and column-level structured pruning are more hardware-friendly but may overlook critical sparse patterns, leading to degraded accuracy [48]. To balance trade-off, we adopt block-level semi-structured pruning strategy to retain accuracy and improve deployability. Specifically, we partition the positional attention map into several blocks of size  $s \times s$ , where  $s$  is configurable stride size. To accommodate sequences whose length  $n$  can not be divisible by  $s$ , we apply zero-padding to the top and right edges of attention map until the dimension becomes divisible. Since FuXi- $\gamma$  adopts a decoder-only architecture, the upper-triangular region of the attention map is masked with 0. Therefore, our padding operation does not damage the original meaningful information.

**3.5.2 Leftmost Importance Scoring.** An effective scoring method should robustly identify the high-utility regions of attention map while maintaining computational efficiency. To this end, we propose the leftmost scoring method as shown in Figure 2. Given that attention map reflects contribution through weighted summation, we use the sum of absolute values within each block as a proxy for importance. To reduce computation, we utilize the persymmetry of Toeplitz matrix:  $W_{pos}^{i,j} = W_{pos}^{i+m,j+m}$ , as established in Section 3.3.1.

This means all blocks lying on the same diagonal share identical values. Consequently, it suffices to compute importance scores only for the blocks in the leftmost column, each of which uniquely represents one diagonal slice of the entire map. Our scoring method is effective for two key reasons: (1) Coverage Guarantee: Since each positional weight is included in at least one leftmost block, the scoring process ensures full coverage of attention weights. (2) Structural Awareness: The leftmost column intersects with all slash-like patterns (i.e., diagonals), enabling efficient detection of meaningful structures and guiding sparse attention accordingly.

**3.5.3 Diagonal-Sliding Selection.** Based on importance scores, we propose a diagonal-sliding block selection method to generate the final sparse attention mask. The formal algorithm is summarized in Algorithm 1. Let  $n$  denote the sequence length,  $s$  the configured stride size, and  $\tau \in [0, 1]$  the configured pruning ratio. After estimating the importance scores of  $\frac{n}{s}$  leftmost blocks, we identify the top- $k$  most unimportant blocks, where  $k = \lfloor \frac{n}{s} \cdot \tau \rfloor$ . Then, we slide these identified blocks diagonally across the entire attention map to generate final sparse mask. This overall sparsity mechanism effectively and efficiently identifies and prunes redundant blocks within the positional attention map in a diagonally structured manner.

---

#### Algorithm 1: Diagonal-Sliding Sparse Mask Generation

---

**Input:** Positional attention map  $W_{pos} \in \mathbb{R}^{n \times n}$ ; Stride size  $s$ ; Pruning ratio  $\tau$   
**Output:** Sparse mask  $M$

```

1 Block Division:
2  $num\_blocks \leftarrow \frac{n}{s}$ 
3  $leftmost\_blocks \leftarrow W_{pos}[:, :s].view(num\_blocks, s, s)$ 
4 Leftmost Importance Scoring:
5  $abs\_sum \leftarrow \text{sum}(|leftmost\_blocks|, \text{dim} = (2, 3))$ 
6  $max\_index \leftarrow num\_blocks \times num\_blocks - 1$ 
7  $num\_mask \leftarrow \lfloor num\_blocks \times \tau \rfloor$ 
8  $\_, indices\_to\_mask \leftarrow \text{TopK}(abs\_sum, k = num\_mask, \text{largest} = \text{False})$ 
9  $real\_indices \leftarrow indices\_to\_mask \times num\_blocks$ 
10 Diagonal-Sliding Selection:
11  $M \leftarrow []$ 
12  $increment \leftarrow num\_blocks + 1$ 
13 foreach  $index \in real\_indices$  do
14   while  $index \leq max\_index$  do
15      $M.append(index)$ 
16      $index \leftarrow index + increment$ 
17   end
18 end
19 return  $M$ 

```

---

## 4 Experiment

### 4.1 Experimental Setup

**Table 1: Statistics of the datasets.**

Datasets	#Users	#Items	#Actions	Avg. Len.
ML-1M	6,040	3,706	1,000,209	165.60
ML-20M	138,493	26,744	20,000,263	144.41
KuaiRand	25,634	7,550	1,432,897	55.90
Industrial	28,927,689	476,544	1,313,729,225	45.41

**4.1.1 Datasets.** To evaluate the performance of our FuXi- $\gamma$ , we conduct experiments on four real-world datasets, including three public datasets and one large-scale industrial dataset. These datasets involve three different scenarios, including movie, video, and music.

**Table 2: Overall recommendation performance comparison on the public datasets. The best result is highlighted in bold, and the second-best result is underlined. Superscript \* indicates the statistically significant improvements (i.e., two-sided t-test with  $p < 0.05$ ). NG@10 and NG@50 stand for NDCG@10 and NDCG@50, respectively. Infer. denotes the inference latency: we normalize our FuXi- $\gamma$ 's latency to 1.00, and report the latencies of all other models as multiples relative to FuXi- $\gamma$ .**

Model	ML-1M					ML-20M						KuaiRand				
	HR@10	HR@50	NG@10	NG@50	MRR	HR@10	HR@50	NG@10	NG@50	MRR	Infer.	HR@10	HR@50	NG@10	NG@50	MRR
LinRec	0.2374	0.4923	0.1301	0.1860	0.1124	0.1629	0.3950	0.0845	0.1350	0.0748	0.98	0.0799	0.2454	0.0396	0.0750	0.0382
FLASH	0.2731	0.5391	0.1506	0.2096	0.1288	0.2484	0.5028	0.1368	0.1928	0.1179	1.26	0.0977	0.2844	0.0495	0.0896	0.0468
GRU4Rec	0.2840	0.5460	0.1551	0.2130	0.1311	0.2411	0.4987	0.1311	0.1877	0.1128	1.00	0.0954	0.2686	0.0482	0.0854	0.0452
SASRec	0.2832	0.5478	0.1583	0.2170	0.1360	0.2645	0.5225	0.1465	0.2033	0.1257	1.05	0.1003	0.2878	0.0505	0.0909	0.0475
LRURec	0.2910	0.5550	0.1641	0.2227	0.1409	0.2732	0.5326	0.1514	0.2086	0.1295	1.21	0.0825	0.2391	0.0415	0.0751	0.0394
Mamba4Rec	0.3140	0.5775	0.1766	0.2351	0.1500	0.2889	0.5491	0.1619	0.2194	0.1384	1.35	0.0903	0.2560	0.0455	0.0810	0.0427
LLaMa	0.3075	0.5799	0.1704	0.2305	0.1441	0.3045	0.5685	0.1723	0.2306	0.1472	1.26	0.1071	0.3060	0.0542	0.0971	0.0508
HSTU	0.2955	0.5727	0.1667	0.2279	0.1433	0.2929	0.5582	0.1653	0.2239	0.1418	1.27	0.1050	0.2911	0.0535	0.0936	0.0498
FuXi- $\alpha$	0.3205	0.5892	0.1814	0.2409	0.1545	0.3359	0.5971	0.1956	0.2534	0.1677	1.34	0.1108	0.3081	0.0555	0.0981	0.0513
FuXi- $\beta$	0.3207	0.5811	0.1864	0.2443	0.1605	0.3324	0.5909	0.1945	0.2517	0.1673	1.03	0.1064	0.2979	0.0534	0.0946	0.0495
<b>FuXi-<math>\gamma</math></b>	<b>0.3255</b>	<b>0.5928</b>	<b>0.1850</b>	<b>0.2443</b>	<b>0.1576</b>	<b>0.3346</b>	<b>0.5918</b>	<b>0.1960</b>	<b>0.2529</b>	<b>0.1684</b>	<b>1.00</b>	<b>0.1118</b>	<b>0.3082</b>	<b>0.0562</b>	<b>0.0984</b>	<b>0.0518</b>
LinRec-Large	0.0385	0.1301	0.0189	0.0381	0.0200	0.0483	0.1276	0.0235	0.0404	0.0221	0.94	0.0503	0.1153	0.0247	0.0386	0.0223
FLASH-Large	0.2807	0.5464	0.1552	0.2140	0.1324	0.2908	0.5470	0.1639	0.2205	0.1402	1.78	0.0983	0.2852	0.0492	0.0894	0.0464
GRU4Rec-Large	0.2285	0.4857	0.1226	0.1790	0.1054	0.2001	0.4524	0.1048	0.1601	0.0910	1.07	0.0885	0.2463	0.0446	0.0786	0.0419
SASRec-Large	0.0375	0.1303	0.0177	0.0371	0.0186	0.0414	0.1218	0.0207	0.0382	0.0208	1.12	0.0470	0.1054	0.0251	0.0376	0.0233
LRURec-Large	0.0392	0.1325	0.0188	0.0384	0.0195	0.0454	0.1288	0.0225	0.0404	0.0220	1.64	0.0525	0.1201	0.0269	0.0410	0.0242
Mamba4Rec-Large	0.0505	0.1563	0.0253	0.0477	0.0254	0.0441	0.1367	0.0220	0.0418	0.0220	1.64	0.0513	0.1361	0.0268	0.0448	0.0254
LLaMa-Large	0.3259	0.5920	0.1856	0.2450	0.1584	0.3459	0.6069	0.2020	0.2598	0.1730	1.78	0.1073	0.3042	0.0540	0.0964	0.0503
HSTU-Large	0.3293	0.5930	0.1867	0.2454	0.1586	0.3405	0.6007	0.1992	0.2568	0.1710	1.79	0.1065	0.2944	0.0535	0.0938	0.0493
FuXi- $\alpha$ -Large	0.3321	0.5908	0.1919	0.2493	0.1641	0.3535	0.6086	0.2095	0.2660	0.1801	2.03	0.1107	0.3072	0.0552	0.0974	0.0508
FuXi- $\beta$ -Large	0.3390	0.6020	0.1945	0.2529	0.1656	0.3551	0.6106	0.2109	0.2675	0.1814	1.15	0.1079	0.3046	0.0543	0.0966	0.0505
<b>FuXi-<math>\gamma</math>-Large</b>	<b>0.3423*</b>	<b>0.6029*</b>	<b>0.1975*</b>	<b>0.2552*</b>	<b>0.1682*</b>	<b>0.3588*</b>	<b>0.6137*</b>	<b>0.2135*</b>	<b>0.2700*</b>	<b>0.1836*</b>	<b>1.00</b>	<b>0.1137*</b>	<b>0.3162*</b>	<b>0.0571*</b>	<b>0.1006*</b>	<b>0.0525*</b>

For dataset preprocessing, we follow the common practice in [52, 53, 55]. The statistics of the processed datasets are shown in Table 1.

- **MovieLens** [12]: This is a widely used benchmark dataset for evaluating recommendation algorithms. The dataset includes users' rating and tagging activities. In this paper, we adopt two well-established versions for our experiments, i.e., MovieLens-1M (ML-1M<sup>1</sup>) and MovieLens-20M (ML-20M<sup>2</sup>).
- **KuaiRand** [7]: The dataset<sup>3</sup> is collected from sequential interaction logs of Kuaishou, a prominent short-video sharing mobile application. This platform shows high engagement, averaging 50+ interactions per active user.
- **Industrial**: This dataset is constructed from the user records of an industrial mainstream music app, which has tens of millions of active users every month. This complex dataset can better evaluate the robustness and effectiveness of models.

**4.1.2 Baselines.** For a competitive comparison, we evaluate FuXi- $\gamma$  against a broad set of representative baselines spanning diverse architectures, including LinRec [33], FLASH [18], GRU4Rec [16], SASRec [22], LRURec [54], Mamba4Rec [31], LLaMa [10], HSTU [55], FuXi- $\alpha$  [52], and FuXi- $\beta$  [53]. These baselines collectively cover the key and efficient paradigms in modern sequential recommendation, such as RNN-based, Transformer-based, and Mamba-based architectures, ensuring a fair and comprehensive evaluation.

**4.1.3 Evaluation Metrics.** We employ three well-established evaluation metrics to evaluate recommendation performance: Hit Ratio (HR), Normalized Discounted Cumulative Gain (NDCG), and Mean Reciprocal Rank (MRR) [52, 55]. HR@K measures whether the ground-truth item appears within the top-K positions of the recommendation list. NDCG@K evaluates top-K recommendation quality by assigning higher scores to relevant items ranked closer

to the top. MRR evaluates the ranking quality by computing the reciprocal rank of the first relevant item in the recommendation results. For all these metrics, higher values indicate better recommendation performance. Following common practice [52, 53], we report HR@K and NDCG@K with K = 10, 50 by default.

**4.1.4 Implementation Details.** We implement FuXi- $\gamma$  using PyTorch<sup>4</sup>. For fair comparison, all models share the same hyperparameter settings, primarily following FuXi- $\alpha$  [52] and FuXi- $\beta$  [53]. Specifically, we use the AdamW optimizer [35] with a learning rate of 0.001 and a batch size of 128. The hidden dimensions are set to 50, 64, 256, and 256 for ML-1M, KuaiRand, ML-20M, and Industrial datasets, respectively. The dropout rate is set to 0.2, and the number of negative samples is set to 128. For our FuXi- $\gamma$ , the temporal encoder's decay parameter  $\gamma$  is set to 0.8 for movie and video scenarios, and 0.9 for music. This setting reflects the intuition that music consumption typically exhibits stronger long-term user preferences, thus requiring a slower decay rate to preserve long-range interest signals, whereas movie/video interactions are more sensitive to recent behaviors. To evaluate base modeling capacity, we set the number of layers to 2. To analyze scaling effects, we extend the models to 8 layers (i.e., 4× deeper) and denote the variants as "XX-Large". For the Industrial dataset, we adopt 4 layers, consistent with the deployed online model. To enable efficient large-scale training, we utilize multi-NPU parallelism via the Accelerate library [26].

## 4.2 Overall Performance

**4.2.1 Recommendation Performance on Public Datasets.** As shown in Table 2, we summarize the key observations as follows:

- Our proposed FuXi- $\gamma$  consistently outperforms state-of-the-art baselines across all datasets. Under the 8-layer configuration, FuXi- $\gamma$  surpasses other autoregressive models by an average of

<sup>1</sup><https://grouplens.org/datasets/movielens/1m/>

<sup>2</sup><https://grouplens.org/datasets/movielens/20m/>

<sup>3</sup><https://kuairand.com/>

<sup>4</sup><https://pytorch.org/>



3.79% in HR@10, 2.37% in HR@50, 4.46% in NDCG@10, 3.49% in NDCG@50, and 4.24% in MRR. Even with shallow 2-layer configuration, FuXi- $\gamma$  still achieves the best or second-best performance, demonstrating its strong ability to capture user interest patterns. Notably, our proposed exponential-power temporal encoder contributes meaningfully to this improvement. An in-depth study of this module is provided in Section 4.3.

- Generative models based on autoregressive architectures overall outperform the traditional methods, which aligns with previous findings [11, 49, 52, 53, 55]. For example, increasing the depth of GRU4Rec or SASRec from 2 to 8 layers results in performance degradation, indicating that traditional architectures struggle to model complex item dependencies. In contrast, generative models exhibit strong scaling effects, highlighting their potential for more expressive sequence recommendation modeling.
- Our FuXi- $\gamma$  achieves excellent inference efficiency, surpassed only by LinRec on ML-20M. The efficiency gains primarily stem from three factors: (1) Nearly pure matrix-based architecture: Each FuXi- $\gamma$  block consists almost entirely of hardware-friendly matrix operations, enabling high hardware utilization. (2) Minimalistic single-head attention: FuXi- $\gamma$  employs no query-key attention and no multi-head expansion, avoiding the costly projections, scaling operations, activations, head-wise computations, and tensor-splitting overheads typical of Transformers. (3) Efficient temporal encoder: The exponential-power temporal encoder relies on continuous matrix operations rather than discrete bucket lookups, eliminating irregular memory access. Further evaluation of efficiency against strong generative baselines across varying sequence lengths is provided in Section 4.2.4.

**Table 3: Overall recommendation performance comparison on the industrial dataset. The best result is highlighted in bold, and the second-best result is underlined. Superscript \* indicates the statistically significant improvements (i.e., two-sided t-test with  $p < 0.05$ ).**

Model	Industrial				
	HR@10	HR@50	NG@10	NG@50	MRR
SASRec	0.2954	0.5742	0.1633	0.2256	0.1397
LLaMa	0.3714	0.6231	0.2216	0.2779	0.1907
HSTU	0.3831	0.6336	0.2294	0.2855	0.1972
FuXi- $\alpha$	0.4060	0.6483	0.2479	0.3022	0.2137
FuXi- $\beta$	0.4734	0.6776	0.3174	0.3633	0.2811
<b>FuXi-<math>\gamma</math></b>	<b>0.5064*</b>	<b>0.6894*</b>	<b>0.3559*</b>	<b>0.3969*</b>	<b>0.3196*</b>

**4.2.2 Recommendation Performance on Industrial Dataset.** As shown in Table 3, FuXi- $\gamma$  shows more significant advantages on our large-scale industrial music dataset. Compared with other autoregressive baselines, it achieves **25.06%** higher HR@10 and **42.86%** higher NDCG@10 on average. Against the strongest baseline FuXi- $\beta$ , our FuXi- $\gamma$  achieves gains of 6.97% in HR@10, 1.74% in HR@50, 12.13% in NDCG@10, 9.25% in NDCG@50, and 13.70% in MRR. These results further demonstrate that FuXi- $\gamma$  generalizes well in various application scenarios, benefiting from our temporal encoder that adaptively models both long-term and short-term user interests.

**4.2.3 Ablation Study.** Table 4 reports the results of ablation studies on the three public datasets. Among all components, our proposed exponential-power temporal encoder proves to be the most critical.

It allows the model to assign differentiated weights to items based on time intervals, effectively capturing the temporal evolution of user preferences. The positional encoder contributes moderately. Since item representations already incorporate absolute positional embeddings, and temporal information implicitly encodes sequential order, the relative positional channel provides marginal yet complementary gains. The SwiGLU FFN’s impact is relatively minor, suggesting that FuXi- $\gamma$ ’s dual-channel self-attention layer sufficiently models sequence dependencies. Nevertheless, its implicit interaction provides a minor boost to model expressiveness.

**Table 4: Ablation study based on FuXi- $\gamma$ .**

Setting	ML-1M		ML-20M		KuaiRand	
	HR@10	NG@10	HR@10	NG@10	HR@10	NG@10
<b>FuXi-<math>\gamma</math></b>	<b>0.3423</b>	<b>0.1975</b>	<b>0.3588</b>	<b>0.2135</b>	<b>0.1137</b>	<b>0.0571</b>
w/o SwiGLU FFN	0.3361	0.1931	0.3496	0.2059	0.1117	0.0570
w/o Positional Encoder	0.3281	0.1865	0.3548	0.2096	0.1113	0.0559
w/o Temporal Encoder	0.3120	0.1767	0.3248	0.1882	0.1043	0.0521

**4.2.4 Efficiency Performance.** Having established the effectiveness of FuXi- $\gamma$ , we now evaluate its computational efficiency across varying sequence lengths. Comparisons are made against other autoregressive generative models, which uniformly outperform traditional baselines in both accuracy and scaling effects. We report results on KuaiRand, with consistent trends observed across other datasets. (1) Training Efficiency: As shown in Figure 3(a), FuXi- $\gamma$  stably achieves the highest training efficiency across all sequence lengths, with its advantage growing more pronounced at longer sequences. At a length of 1000, it achieves speedups of **4.74×**, **4.48×**, and **1.86×** over LLaMa, HSTU, and FuXi- $\beta$ , respectively. Notably, FuXi- $\alpha$  encounters out-of-memory (OOM) issue at this scale, due to its computationally intensive three-channel architecture. (2) Inference Efficiency: Figure 3(b) further demonstrates FuXi- $\gamma$ ’s leading inference efficiency, with the performance gap similarly widening at longer sequence lengths. At length 1000, FuXi- $\gamma$  achieves inference speedups of **6.18×**, **6.07×**, and **2.24×** over LLaMa, HSTU, and FuXi- $\beta$ , respectively. These results underscore FuXi- $\gamma$ ’s strong scalability and practical suitability for long-sequence recommendation, attributed to its streamlined dual-channel architecture and lightweight exponential-power temporal encoder.

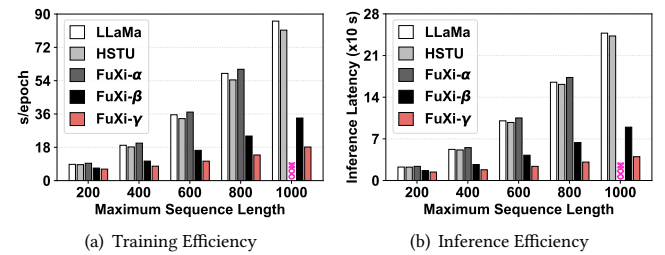


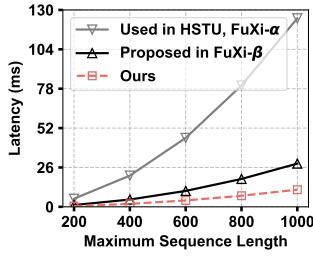
**Figure 3: Overall efficiency performance comparison.**

### 4.3 Study of Temporal Encoder

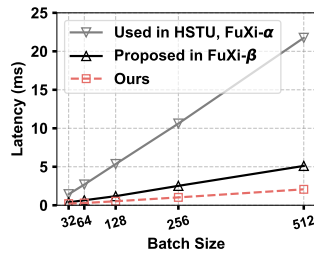
**4.3.1 Compatibility.** As shown in Table 5, we evaluate the compatibility of different temporal encoders by integrating them into three representative state-of-the-art architectures. Our exponential-power temporal encoder robustly yields the highest accuracy improvements across all architectures on all datasets. On average,

Table 5: Compatibility comparison of temporal encoders.

Architecture	Temporal Encoder	ML-1M			ML-20M			KuaiRand		
		HR@10	NG@10	MRR	HR@10	NG@10	MRR	HR@10	NG@10	MRR
HSTU	w/o	0.3117	0.1719	0.1444	0.3151	0.1805	0.1544	0.1004	0.0502	0.0465
	Used in HSTU, FuXi- $\alpha$	0.3293	0.1867	0.1586	0.3405	0.1992	0.1710	0.1065	0.0535	0.0493
	Proposed in FuXi- $\beta$	0.3224	0.1853	0.1589	0.3410	0.1995	0.1713	0.1048	0.0530	0.0492
	Ours	<b>0.3312</b>	<b>0.1897</b>	<b>0.1618</b>	<b>0.3426</b>	<b>0.2012</b>	<b>0.1729</b>	<b>0.1084</b>	<b>0.0551</b>	<b>0.0513</b>
FuXi- $\alpha$	w/o	0.3104	0.1738	0.1476	0.3226	0.1870	0.1602	0.1020	0.0515	0.0483
	Used in HSTU, FuXi- $\alpha$	0.3321	0.1919	0.1641	0.3535	0.2095	0.1801	0.1107	0.0552	0.0508
	Proposed in FuXi- $\beta$	0.3338	0.1891	0.1599	0.3538	0.2098	0.1803	0.1071	0.0539	0.0500
	Ours	<b>0.3361</b>	<b>0.1940</b>	<b>0.1657</b>	<b>0.3540</b>	<b>0.2104</b>	<b>0.1810</b>	<b>0.1114</b>	<b>0.0566</b>	<b>0.0520</b>
FuXi- $\gamma$ , FuXi- $\beta$	w/o	0.3120	0.1767	0.1508	0.3248	0.1882	0.1611	0.1043	0.0521	0.0488
	Used in HSTU, FuXi- $\alpha$	0.3350	0.1931	0.1655	0.3550	0.2107	0.1811	0.1111	0.0557	0.0512
	Proposed in FuXi- $\beta$	0.3390	0.1945	0.1656	0.3551	0.2109	0.1814	0.1079	0.0543	0.0505
	Ours	<b>0.3423</b>	<b>0.1975</b>	<b>0.1682</b>	<b>0.3588</b>	<b>0.2135</b>	<b>0.1836</b>	<b>0.1137</b>	<b>0.0571</b>	<b>0.0525</b>



(a) Under Different Max. Seq. Lengths



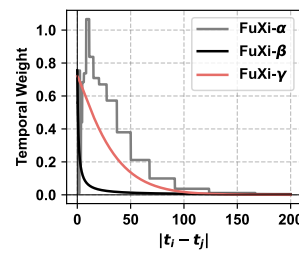
(b) Under Different Batch Sizes

Figure 4: Efficiency comparison of temporal encoders.

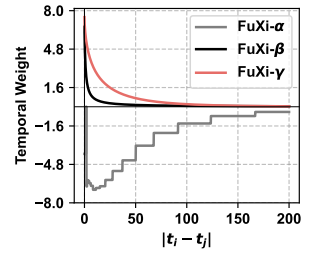
it improves HR@10, NDCG@10, and MRR by 8.82%, 11.16%, and 11.15%, respectively, compared to the non-temporal baseline. This performance gain stems from its alignment with human memory decay patterns via exponential modeling. In addition, the temporal encoders used in HSTU, FuXi- $\alpha$ , and FuXi- $\beta$  also lead to varying degrees of improvement, reaffirming the critical role of temporal modeling in sequential recommendation task.

**4.3.2 Efficiency.** Figure 4 presents a comparative analysis of the computational efficiency of our exponential-power temporal encoder against two strong baselines. Across all sequence lengths, our encoder achieves the lowest latency, owing to its continuous memory access pattern, lightweight computation, and pre-conversion of data type. In contrast, bucket-based encoder (e.g., adopted by HSTU and FuXi- $\alpha$ ) exhibits severe degradation in efficiency as sequence length increases. This is primarily due to their discontinuous memory addressing, which is fundamentally incompatible with modern parallel hardware architectures. Although FuXi- $\beta$  improves upon this with an inverse-proportional decay function, it still falls short of our method. At a sequence length of 1000, our encoder achieves **11.00×** and **2.52×** speedup over two baselines, respectively. Furthermore, while the latency of all encoders scales proportionally with batch size, ours reliably maintains superior efficiency.

**4.3.3 Visualization.** Figure 5 illustrates the encoding patterns of different temporal encoders. The horizontal axis represents the relative time interval between two items, and the vertical axis denotes the corresponding attention weight assigned. We visualize the first-layer temporal encoders of FuXi- $\alpha$ , FuXi- $\beta$ , and FuXi- $\gamma$  trained on ML-1M and ML-20M. All encoders follow the intuitive pattern that

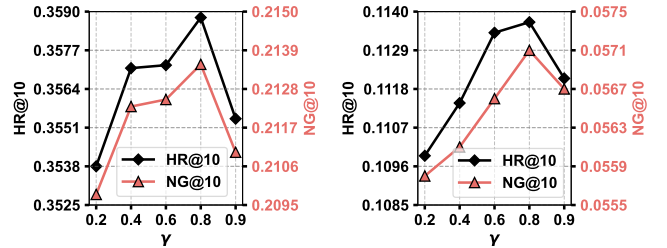


(a) Layer-1 on ML-1M

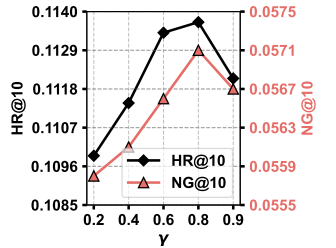


(b) Layer-1 on ML-20M

Figure 5: Visualization comparison of temporal encoders.



(a) On ML-20M



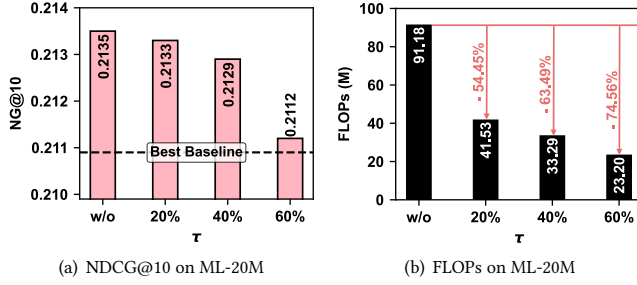
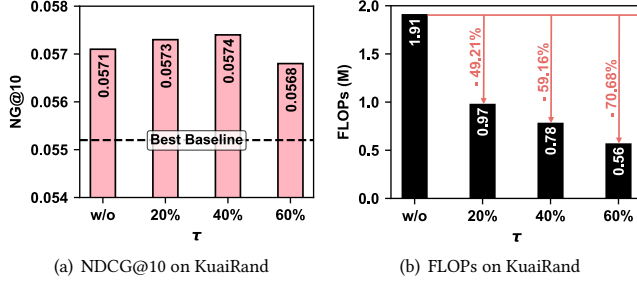
(b) On KuaiRand

Figure 6: Hyper-parameter study of  $\gamma$ .

longer intervals receive lower weights, emphasizing the importance of recent interactions. FuXi- $\beta$  exhibits a steep initial decline, allocating excessive weights to very short-term intervals and limiting long-range modeling. FuXi- $\alpha$  shows a sawtooth pattern, caused by its bucketization strategy, where multiple time intervals are mapped to the same bucket, and adjacent buckets are not smoothly connected. In contrast, our FuXi- $\gamma$  generates a smooth, continuous decay curve, thanks to its exponential-power function design. This allows it to differentiate both short- and long-term intervals.

**4.3.4 Impact of Hyper-Parameter  $\gamma$ .** Figure 6 presents the impact of the decay-rate hyper-parameter  $\gamma$  on model performance in two domains: movie and video. As  $\gamma$  increases, temporal decay becomes slower. We observe that  $\gamma = 0.8$  achieves the best performance in both domains, balancing the preservation of long-term preferences with sensitivity to short-term variations. A too-fast decay (e.g., smaller  $\gamma$ ) weakens long-range signals, while a too-slow decay



Figure 7: Impact of configured pruning ratio  $\tau$  on ML-20M.Figure 8: Impact of configured pruning ratio  $\tau$  on KuaiRand.

(e.g., larger  $\gamma$ ) dilutes recent behavior effects. As mentioned in Section 4.1.4, we achieve the best results on our industrial music dataset with  $\gamma = 0.9$ , aligning with the domain characteristic that music preferences are more persistent and long-term oriented.

#### 4.4 Study of Sparse Positional Mechanism

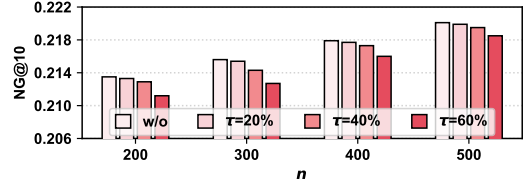
Although FuXi- $\gamma$  already exhibits strong efficiency, we further investigate deployment-oriented optimizations by introducing the diagonal-sparse positional mechanism. We evaluate its effects on both effectiveness and efficiency across three representative scenarios: ML-20M (movie), KuaiRand (video), and Industrial (music).

**4.4.1 Impact of Configured Pruning Ratio  $\tau$ .** As shown in Figure 7, on ML-20M, increasing the pruning ratio  $\tau$  leads to a mild and acceptable accuracy drop. Even at  $\tau = 60\%$ , FuXi- $\gamma$  retains 98.92% of its original accuracy, still outperforming the strongest competing baseline. Meanwhile, the FLOPs of positional attention are reduced by 74.56%, highlighting substantial computational savings. As shown in Figure 8, on KuaiRand, we observe a slight accuracy improvement at moderate sparsity levels, suggesting that pruning redundant attention blocks can even enhance generalization. At  $\tau = 60\%$ , NDCG@10 decreases by only 0.53%, while FLOPs are reduced by 70.68%. As shown in Figure 12 in Appendix C, on Industrial, the sparsity mechanism incurs almost no accuracy loss, substantially improving its deployability. These results confirm that our semi-structured pruning method effectively eliminates redundancy in positional attention while retaining critical information.

**4.4.2 Impact of Stride Size  $s$ .** Table 6 summarizes the effect of varying stride size  $s$  on accuracy and parameter density, using ML-20M as a representative dataset. The results show that  $s = 8$  offers the best trade-off, achieving strong accuracy with relatively low parameter density. Smaller  $s$  leads to finer-grained block division, enabling

Table 6: Impact of stride size  $s$  on ML-20M.

Stride	$s=4$	$s=8$	$s=16$	$s=32$
HR@10	0.3574	0.3576	0.3556	0.3567
NG@10	0.2126	0.2129	0.2115	0.2119
Density	33.14%	33.29%	33.47%	36.84%

Figure 9: Impact of sequence length  $n$  on ML-20M.

more precise sparsity, but it narrows the scoring range and limits parallelism due to fragmented block structures. In contrast, larger  $s$  results in coarse-grained blocks, which reduces the effectiveness of sparsity and may fail to capture fine-grained redundancy. Thus, the stride size should be adaptively selected based on the deployment context to balance accuracy, density, and efficiency.

**4.4.3 Impact of Sequence Length  $n$ .** Figure 9 summarizes the robustness of our sparsity mechanism across different sequence lengths, using ML-20M as a representative dataset. The results show that the method remains uniformly stable: even at  $\tau = 60\%$ , FuXi- $\gamma$  preserves over 98.65% of its original accuracy, and the performance drop further diminishes as the sequences become longer. This trend suggests that longer input sequences may contain higher redundancy in positional interactions, making them more amenable to pruning. Consequently, our pruning method holds greater potential for practical deployment in long-sequence recommender systems.

## 5 Conclusion

In this paper, we propose a novel sequential recommendation framework, named FuXi- $\gamma$ , to address the dual challenges of efficiency and effectiveness in modeling user interests. Our FuXi- $\gamma$  introduces two core innovations: Exponential-Power Temporal Encoder and Diagonal-Sparse Positional Mechanism. Exponential-power temporal encoder is inspired by cognitive memory theory and involves only standard matrix operations, enabling it to flexibly capture both short-term and long-term user interests while ensuring efficient execution on modern hardware. Diagonal-sparse positional mechanism employs a diagonally semi-structured manner to effectively identify and prune redundant attention blocks, thereby reducing computational cost while preserving recommendation quality. Extensive experiments on four real-world datasets demonstrate that our proposed FuXi- $\gamma$  consistently outperforms state-of-the-art baselines in both recommendation accuracy and computational efficiency. In future work, we plan to further improve the efficiency and extend the framework to capture more complex user behavior patterns.

## Acknowledgments

This work is supported by the National Natural Science Foundation of China (62372253), the Natural Science Foundation of Tianjin Fund (23JCYBJC00010), and Nankai University School of Optometry and Vision Science Open Fund Program (NKSGP202308). The work is also sponsored by Huawei Innovation Research Program.

## References

- [1] Junyi Chen, Lu Chi, Bingyue Peng, and Zehuan Yuan. 2024. Hllm: Enhancing sequential recommendations via hierarchical large language models for item and user modeling. *arXiv preprint arXiv:2409.12740* (2024).
- [2] Sung Min Cho, Eunhyeok Park, and Sungjoo Yoo. 2020. MEANTIME: Mixture of attention mechanisms with multi-temporal embeddings for sequential recommendation. In *Proceedings of the 14th ACM Conference on recommender systems*. 515–520.
- [3] Zihang Dai, Zhilin Yang, Yiming Yang, Jaime Carbonell, Quoc V Le, and Ruslan Salakhutdinov. 2019. Transformer-xl: Attentive language models beyond a fixed-length context. *arXiv preprint arXiv:1901.02860* (2019).
- [4] Tri Dao and Albert Gu. 2024. Transformers are ssms: Generalized models and efficient algorithms through structured state space duality. *arXiv preprint arXiv:2405.21060* (2024).
- [5] Hermann Ebbinghaus. 1885. Memory: a contribution to experimental psychology. teachers college, columbia university, new york. *Trans. HA Ruger and CE Busenius. Original work published* (1885).
- [6] Stefan Elfving, Eiji Uchibe, and Kenji Doya. 2018. Sigmoid-weighted linear units for neural network function approximation in reinforcement learning. *Neural networks* 107 (2018), 3–11.
- [7] Chongming Gao, Shijun Li, Yuan Zhang, Jiawei Chen, Biao Li, Wenqiang Lei, Peng Jiang, and Xiangnan He. 2022. KuaiRand: An Unbiased Sequential Recommendation Dataset with Randomly Exposed Videos. In *Proceedings of the 31st ACM International Conference on Information and Knowledge Management* (Atlanta, GA, USA) (CIKM '22). 3953–3957. doi:10.1145/3511808.3557624
- [8] Yizhao Gao, Zhichen Zeng, Dayou Du, Shijie Cao, Peiyuan Zhou, Jiaxing Qi, Junjie Lai, Hayden Kwok-Hay So, Ting Cao, Fan Yang, et al. 2024. Seerattention: Learning intrinsic sparse attention in your llms. *arXiv preprint arXiv:2410.13276* (2024).
- [9] Jonas Gehring, Michael Auli, David Grangier, Denis Yarats, and Yann N Dauphin. 2017. Convolutional sequence to sequence learning. In *International conference on machine learning*. PMLR, 1243–1252.
- [10] Aaron Grattafiori, Abhimanyu Dubey, Abhinav Jauhri, Abhinav Pandey, Abhishek Kadian, Ahmad Al-Dahle, Aiesha Letman, Akhil Mathur, Alan Schelten, Alex Vaughan, et al. 2024. The llama 3 herd of models. *arXiv preprint arXiv:2407.21783* (2024).
- [11] Wei Guo, Hao Wang, Luankang Zhang, Jin Yao Chin, Zhongzhou Liu, Kai Cheng, Qiushi Pan, Yi Quan Lee, Wanqi Xue, Tingjia Shen, et al. 2024. Scaling new frontiers: Insights into large recommendation models. *arXiv preprint arXiv:2412.00714* (2024).
- [12] F Maxwell Harper and Joseph A Konstan. 2015. The movielens datasets: History and context. *Acm transactions on interactive intelligent systems (tiis)* 5, 4 (2015), 1–19.
- [13] Kaiming He, Xiangyu Zhang, Shaoqing Ren, and Jian Sun. 2016. Deep residual learning for image recognition. In *Proceedings of the IEEE conference on computer vision and pattern recognition*. 770–778.
- [14] Pengcheng He, Xiaodong Liu, Jianfeng Gao, and Weizhu Chen. 2020. DeBERTa: Decoding-enhanced bert with disentangled attention. *arXiv preprint arXiv:2006.03654* (2020).
- [15] Ruining He and Julian McAuley. 2016. Fusing similarity models with markov chains for sparse sequential recommendation. In *2016 IEEE 16th international conference on data mining (ICDM)*. IEEE, 191–200.
- [16] Balázs Hidasi, Alexandros Karatzoglou, Linas Baltrunas, and Domonkos Tikk. 2015. Session-based recommendations with recurrent neural networks. *arXiv preprint arXiv:1511.06939* (2015).
- [17] Haoji Hu, Xiangnan He, Jinyang Gao, and Zhi-Li Zhang. 2020. Modeling personalized item frequency information for next-basket recommendation. In *Proceedings of the 43rd international ACM SIGIR conference on research and development in information retrieval*. 1071–1080.
- [18] Weizhe Hua, Zihang Dai, Hanxiao Liu, and Quoc Le. 2022. Transformer quality in linear time. In *International conference on machine learning*. PMLR, 9099–9117.
- [19] Zhiheng Huang, Davis Liang, Peng Xu, and Bing Xiang. 2020. Improve transformer models with better relative position embeddings. *arXiv preprint arXiv:2009.13658* (2020).
- [20] Huiqiang Jiang, Yucheng Li, Chengruidong Zhang, Qianhui Wu, Xufang Luo, Surin Ahn, Zhenhua Han, Amir H Abdi, Dongsheng Li, Chin-Yew Lin, et al. 2024. Minference 1.0: Accelerating pre-filling for long-context llms via dynamic sparse attention. *Advances in Neural Information Processing Systems* 37 (2024), 52481–52515.
- [21] Eija Kaasinen, Virpi Roto, Kristin Roloff, Kaisa Väänänen-Vainio-Mattila, Teija Vainio, Wolfgang Maehr, Dhaval Joshi, and Sujun Shrestha. 2009. User experience of mobile internet: analysis and recommendations. *International Journal of Mobile Human Computer Interaction (IJMHCI)* 1, 4 (2009), 4–23.
- [22] Wang-Cheng Kang and Julian McAuley. 2018. Self-attentive sequential recommendation. In *2018 IEEE international conference on data mining (ICDM)*. IEEE, 197–206.
- [23] Seyed Mehran Kazemi, Rishab Goel, Sepehr Eghbali, Janahan Ramanan, Jaspreet Sahota, Sanjay Thakur, Stella Wu, Cathal Smyth, Pascal Poupart, and Marcus Brubaker. 2019. Time2vec: Learning a vector representation of time. *arXiv preprint arXiv:1907.05321* (2019).
- [24] Guolin Ke, Di He, and Tie-Yan Liu. 2020. Rethinking positional encoding in language pre-training. *arXiv preprint arXiv:2006.15595* (2020).
- [25] Anton Klenitskiy and Alexey Vasilev. 2023. Turning dross into gold loss: is bert4rec really better than sasrec?. In *Proceedings of the 17th ACM Conference on Recommender Systems*. 1120–1125.
- [26] John P Kotter. 2012. Accelerate. *Harvard business review* 90, 11 (2012), 43–58.
- [27] Xunhao Lai, Jianqiao Lu, Yao Luo, Yiyuan Ma, and Xun Zhou. 2025. Flexprell: A context-aware sparse attention mechanism for efficient long-sequence inference. *arXiv preprint arXiv:2502.20766* (2025).
- [28] Jiacheng Li, Yujie Wang, and Julian McAuley. 2020. Time interval aware self-attention for sequential recommendation. In *Proceedings of the 13th international conference on web search and data mining*. 322–330.
- [29] Jun Li and Ge Zhang. 2023. Fragment and Integrate Network (FIN): A Novel Spatial-Temporal Modeling Based on Long Sequential Behavior for Online Food Ordering Click-Through Rate Prediction. In *Proceedings of the 32nd ACM International Conference on Information and Knowledge Management*. 4688–4694.
- [30] Xiangyang Li, Bo Chen, Lu Hou, and Ruiming Tang. 2023. Ctrl: Connect tabular and language model for ctr prediction. *arXiv preprint arXiv:2306.02841* (2023).
- [31] Chengkai Liu, Jianghao Lin, Jianling Wang, Hanzhou Liu, and James Caverlee. 2024. Mamba4rec: Towards efficient sequential recommendation with selective state space models. *arXiv preprint arXiv:2403.03900* (2024).
- [32] Hu Liu, Jing Lu, Hao Yang, Xiwei Zhao, Sulong Xu, Hao Peng, Zehua Zhang, Wenjie Niu, Xiaokun Zhu, Yongjun Bao, et al. 2020. Category-Specific CNN for Visual-aware CTR Prediction at JD. com. In *Proceedings of the 26th ACM SIGKDD international conference on knowledge discovery & data mining*. 2686–2696.
- [33] Langming Liu, Liu Cai, Chi Zhang, Xiangyu Zhao, Jingtong Gao, Wanyu Wang, Yifu Lv, Wenqi Fan, Yiqi Wang, Ming He, et al. 2023. Linrec: Linear attention mechanism for long-term sequential recommender systems. In *Proceedings of the 46th International ACM SIGIR Conference on Research and Development in Information Retrieval*. 289–299.
- [34] Qiang Liu, Shu Wu, Diyi Wang, Zhaokang Li, and Liang Wang. 2016. Context-aware sequential recommendation. In *2016 IEEE 16th International Conference on Data Mining (ICDM)*. IEEE, 1053–1058.
- [35] Ilya Loshchilov and Frank Hutter. 2017. Decoupled weight decay regularization. *arXiv preprint arXiv:1711.05101* (2017).
- [36] Saptarshi Mitra, Rachid Karami, Haocheng Xu, Sitao Huang, and Hyoukjun Kwon. 2025. Characterizing state space model (ssm) and ssm-transformer hybrid language model performance with long context length. *arXiv preprint arXiv:2507.12442* (2025).
- [37] Colin Raffel, Noam Shazeer, Adam Roberts, Katherine Lee, Sharan Narang, Michael Matena, Yanqi Zhou, Wei Li, and Peter J Liu. 2020. Exploring the limits of transfer learning with a unified text-to-text transformer. *Journal of machine learning research* 21, 140 (2020), 1–67.
- [38] Shashank Rajput, Nikhil Mehta, Anima Singh, Raghunandan Hulikal Keshavan, Trung Vu, Lukasz Heldt, Lichan Hong, Yi Tay, Vinh Tran, Jonah Samost, et al. 2023. Recommender systems with generative retrieval. *Advances in Neural Information Processing Systems* 36 (2023), 10299–10315.
- [39] Steffen Rendle, Christoph Freudenthaler, and Lars Schmidt-Thieme. 2010. Factorizing personalized markov chains for next-basket recommendation. In *Proceedings of the 19th international conference on World wide web*. 811–820.
- [40] Peter Shaw, Jakob Uszkoreit, and Ashish Vaswani. 2018. Self-attention with relative position representations. *arXiv preprint arXiv:1803.02155* (2018).
- [41] Noam Shazeer. 2020. Glue variants improve transformer. *arXiv preprint arXiv:2002.05202* (2020).
- [42] Jiajie Su, Chaochao Chen, Zibin Lin, Xi Li, Weiming Liu, and Xiaolin Zheng. 2023. Personalized behavior-aware transformer for multi-behavior sequential recommendation. In *Proceedings of the 31st ACM international conference on multimedia*. 6321–6331.
- [43] Fei Sun, Jun Liu, Jian Wu, Changhua Pei, Xiao Lin, Wenwu Ou, and Peng Jiang. 2019. BERT4Rec: Sequential recommendation with bidirectional encoder representations from transformer. In *Proceedings of the 28th ACM international conference on information and knowledge management*. 1441–1450.
- [44] Jiayi Tang and Ke Wang. 2018. Personalized top-n sequential recommendation via convolutional sequence embedding. In *Proceedings of the eleventh ACM international conference on web search and data mining*. 565–573.
- [45] Ashish Vaswani, Noam Shazeer, Niki Parmar, Jakob Uszkoreit, Llion Jones, Aidan N Gomez, Łukasz Kaiser, and Illia Polosukhin. 2017. Attention is all you need. *Advances in neural information processing systems* 30 (2017).
- [46] Dong Wang, Kavé Salamatian, Yunqing Xia, Weiwei Deng, and Qi Zhang. 2023. BERT4CTR: An Efficient Framework to Combine Pre-trained Language Model with Non-textual Features for CTR Prediction. In *Proceedings of the 29th ACM SIGKDD Conference on Knowledge Discovery and Data Mining*. 5039–5050.
- [47] Xinfei Wang. 2020. A survey of online advertising click-through rate prediction models. In *2020 IEEE International Conference on Information Technology, Big Data*

- and Artificial Intelligence (ICIBA), Vol. 1. IEEE, 516–521.
- [48] Kunpeng Xie, Ye Lu, Xinyu He, Dezhi Yi, Huijuan Dong, and Yao Chen. 2024. Winols: A large-tiling sparse winograd CNN accelerator on FPGAs. *ACM Transactions on Architecture and Code Optimization* 21, 2 (2024), 1–24.
  - [49] Wenjia Xie, Hao Wang, Minghao Fang, Ruize Yu, Wei Guo, Yong Liu, Defu Lian, and Enhong Chen. 2025. Breaking the Bottleneck: User-Specific Optimization and Real-Time Inference Integration for Sequential Recommendation. In *Proceedings of the 31st ACM SIGKDD Conference on Knowledge Discovery and Data Mining* V. 2. 3333–3343.
  - [50] Ruyi Xu, Guangxuan Xiao, Haofeng Huang, Junxian Guo, and Song Han. 2025. Xattention: Block sparse attention with antidiagonal scoring. *arXiv preprint arXiv:2503.16428* (2025).
  - [51] Wenwen Ye, Shuaiqiang Wang, Xu Chen, Xuepeng Wang, Zheng Qin, and Dawei Yin. 2020. Time matters: Sequential recommendation with complex temporal information. In *Proceedings of the 43rd international ACM SIGIR conference on research and development in information retrieval*. 1459–1468.
  - [52] Yufei Ye, Wei Guo, Jin Yao Chin, Hao Wang, Hong Zhu, Xi Lin, Yuyang Ye, Yong Liu, Ruiming Tang, Defu Lian, et al. 2025. FuXi- $\alpha$ : Scaling Recommendation Model with Feature Interaction Enhanced Transformer. In *Companion Proceedings of the ACM on Web Conference 2025*. 557–566.
  - [53] Yufei Ye, Wei Guo, Hao Wang, Hong Zhu, Yuyang Ye, Yong Liu, Hui Feng Guo, Ruiming Tang, Defu Lian, and Enhong Chen. 2025. FuXi- $\beta$ : Towards a light-weight and fast large-scale generative recommendation model. *arXiv preprint arXiv:2508.10615* (2025).
  - [54] Zhenrui Yue, Yueqi Wang, Zhankui He, Huimin Zeng, Julian McAuley, and Dong Wang. 2024. Linear recurrent units for sequential recommendation. In *Proceedings of the 17th ACM international conference on web search and data mining*. 930–938.
  - [55] Jiaqi Zhai, Lucy Liao, Xing Liu, Yueming Wang, Rui Li, Xuan Cao, Leon Gao, Zhaojie Gong, Fangda Gu, Michael He, et al. 2024. Actions speak louder than words: Trillion-parameter sequential transducers for generative recommendations. *arXiv preprint arXiv:2402.17152* (2024).
  - [56] Biao Zhang and Rico Sennrich. 2019. Root mean square layer normalization. *Advances in neural information processing systems* 32 (2019).
  - [57] Lingzi Zhang, Xin Zhou, Zhiwei Zeng, and Zhiqi Shen. 2024. Multimodal pre-training for sequential recommendation via contrastive learning. *ACM Transactions on Recommender Systems* 3, 1 (2024), 1–23.
  - [58] Yin Zhang, Derek Zhiyuan Cheng, Tiansheng Yao, Xinyang Yi, Lichan Hong, and Ed H Chi. 2021. A model of two tales: Dual transfer learning framework for improved long-tail item recommendation. In *Proceedings of the web conference 2021*. 2220–2231.
  - [59] Yihu Zhang, Bo Yang, Haodong Liu, and Dongsheng Li. 2023. A time-aware self-attention based neural network model for sequential recommendation. *Applied Soft Computing* 133 (2023), 109894.
  - [60] Chuang Zhao, Xinyu Li, Ming He, Hongke Zhao, and Jianping Fan. 2023. Sequential recommendation via an adaptive cross-domain knowledge decomposition. In *Proceedings of the 32nd ACM international conference on information and knowledge management*. 3453–3463.

## A Theoretical Discussion of Temporal Encoder

The exponential-power temporal encoder, formulated as

$$f(x) = \alpha \cdot \gamma^{x^\beta}, \quad (8)$$

extends the classical Ebbinghaus forgetting curve into a generalized exponential kernel. Its derivative is

$$f'(x) = \alpha\beta(\ln \gamma)x^{\beta-1}\gamma^{x^\beta}. \quad (9)$$

When  $0 < \beta < 1$ , the term  $x^{\beta-1} = x^{-(1-\beta)}$  diverges as  $x \rightarrow 0$ , violating Lipschitz continuity and potentially introducing optimization instability. To maintain Lipschitz continuity and improve training robustness in this regime, a simple yet effective solution is to shift the input by a small positive constant, replacing  $x$  with  $x + \epsilon$  ( $\epsilon > 0$ ).

## B Analysis of Cold-Start & Sparse-Case

Cold-start users and long-tail items are fundamental sparsity challenges in real-world recommendation systems. To further assess the robustness of FuXi- $\gamma$ , we evaluate model performance under three challenging conditions: (1) cold-start users with very limited interaction histories, (2) fresh items launched within short time windows, and (3) long-tail items with low exposure frequency.

### B.1 Cold-Start Users

We partition the industrial dataset into five groups according to users' historical interaction lengths. As shown in Figure 10, our FuXi- $\gamma$  robustly outperforms all baselines across all user groups, including cold-start users with extremely short sequences. The performance gap becomes even larger for long-sequence users, indicating that the tunable exponential-power temporal encoder effectively captures both short-term and long-term interest patterns.

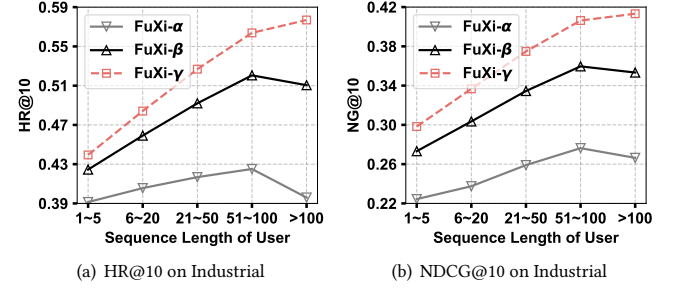


Figure 10: Analysis of cold-start users on Industrial.

### B.2 Fresh Items

We examine the model's ability to recommend fresh items, which lack sufficient historical feedback and are often difficult for models to rank accurately. Following the item-launching-time criterion, we evaluate items introduced within  $\leq 1$  day and  $\leq 1$  week. As shown in Figure 11, FuXi- $\gamma$  achieves the best performance across the two freshness windows. These results highlight FuXi- $\gamma$ 's strong generalization ability to newly introduced content.

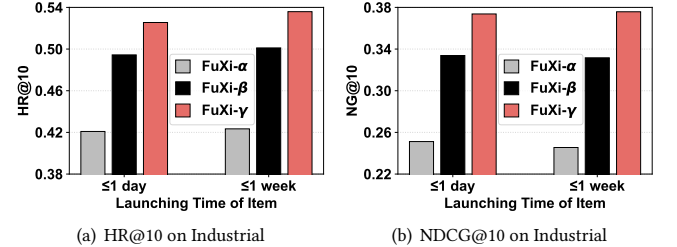


Figure 11: Analysis of fresh items on Industrial.

### B.3 Long-Tail Items

Following [49, 58], we categorize the top 20% most interacted items as head and the remainder as long-tail. As shown in Table 7, FuXi- $\gamma$  stably achieves performance gains over FuXi- $\alpha$  and FuXi- $\beta$  on both subsets. We attribute this advantage to FuXi- $\gamma$ 's fine-grained temporal encoding, which produces richer sequential representations and alleviates embedding sparsity for long-tail items.

Table 7: Analysis of long-tail items on ML-20M.

Model	Head		Tail	
	HR@10	NG@10	HR@10	NG@10
FuXi- $\alpha$	0.3710	0.2205	0.0747	0.0395
FuXi- $\beta$	0.3705	0.2209	0.0756	0.0409
<b>FuXi-<math>\gamma</math></b>	<b>0.3749</b>	<b>0.2234</b>	<b>0.0789</b>	<b>0.0413</b>

### C Supplementary Figure

As described in Section 4.4.1, Figure 12 demonstrates the impact of configured pruning ratio  $\tau$  on Industrial dataset.

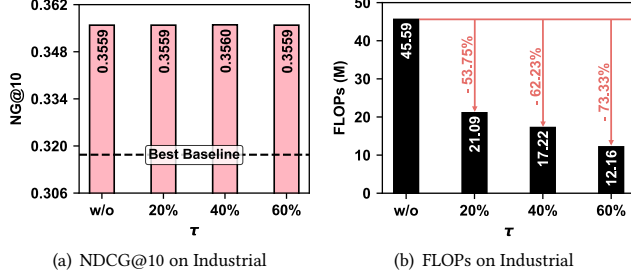


Figure 12: Impact of configured pruning ratio  $\tau$  on Industrial.

### D Efficiency Discussion about Mamba4Rec

As shown in Table 2, on ML-20M, Mamba4Rec is not universally faster, as linear computational complexity does not guarantee superior runtime in all settings. Mamba’s advantage typically emerges for very long sequences (e.g.,  $>2k$ ), while for shorter sequences its efficiency is often lower than that of Transformers [4, 36]. The reason is that achieving linear scaling relies on recurrent state updates, which introduce non-negligible constant computational overhead. In particular, each state update involves complex operations such as matrix multiplications, gating mechanisms, and discretization, requiring additional kernel launches and memory synchronization. These operations exhibit limited parallelism, preventing full utilization of AI accelerators. Consequently, although Mamba avoids the  $O(n^2)$  attention cost, its low hardware parallelism and large constant factors reduce efficiency for typical sequence lengths.